

# AC RESEARCH

## Amide and Ester Surface Attachment Reactions for Alkanethiol Monolayers at Gold Surfaces As Studied by Polarization Modulation Fourier Transform Infrared Spectroscopy

Robert V. Duevel and Robert M. Corn\*

Department of Chemistry, University of Wisconsin, 1101 University Avenue, Madison, Wisconsin 53706

The modification of alkanethiol monolayers via amide and ester formation reactions is demonstrated as a methodology for attaching monolayer and submonolayer coverages of specific chemical species onto metal electrodes. A monolayer of 11-mercaptoundecanoic acid ( $\text{HSC}_{10}\text{H}_{20}\text{COOH}$ ) is used as a surface bifunctional linking agent on polycrystalline gold surfaces. The reaction of these adsorbed molecules with gaseous thionyl chloride converts the carboxylic acid group to an acid chloride which can then be reacted further with an amine or alcohol to form an amide or ester linkage. The attachment of alkyl, aromatic, and electrochemically active species to the surface is reported to demonstrate the versatility of this surface derivatization chemistry. Polarization modulation Fourier transform infrared (PM-FTIR) spectroscopy is employed as the primary method for monitoring the chemical structure of the adsorbed monolayers, and additional X-ray photoelectron spectroscopy (XPS) and electrochemical measurements are used to verify the elemental composition, oxidation state, and surface coverage of the adsorbed molecules.

### INTRODUCTION

The modification of metal surfaces with organic monolayers and thin films is a vast subject that impacts upon a wide variety of technologically and scientifically important areas.<sup>1</sup> The process of spontaneous adsorption and organization of monolayers from dilute solution has been successfully employed with a number of long chain molecules at metal surfaces<sup>2,3</sup> and offers a simple and attractive method of surface modification at the single monolayer level. One of the most successful chemistries employed for spontaneous adsorption and organization at metal surfaces is the attachment of *n*-alkanethiols to gold surfaces.<sup>3</sup> The monolayers formed by these molecules are attracted to the surface by a combination of adsorption and organizational free energies; if the *n*-alkyl chain is sufficiently long, the adsorbed monolayer is extremely robust. An assortment of *n*-alkanethiol monolayers derivatized with a variety of pendant functional groups have been created by a number of research groups in an effort to systematically control the wetting, electrochemical, and photochemical properties of metal surfaces.<sup>4</sup>

Although it is conceivable that any particular molecule can first be prepared and then attached to the surface (assuming

that there are no complicating cross reactions with the thiol group), a very attractive mechanism for creating monolayers with specific chemical, optical, tribological, or electrical properties would be to first adsorb an alkanethiol species onto the surface and subsequently to attach onto the adsorbed monolayer a specific chemical group via a linking reaction. Such linking strategies have been demonstrated previously with aminosilane monolayers and multilayers.<sup>5</sup>

In this paper we verify with infrared reflectance measurements that a linking strategy employing amide and ester formation reactions can be applied to monolayers of carboxylic acid-derivatized long-chain *n*-alkanethiols at gold surfaces. Monolayers of 11-mercaptoundecanoic acid ( $\text{HSC}_{10}\text{H}_{20}\text{COOH}$ ) are reacted via an acid chloride intermediate with a variety of alkyl and aromatic amines to form the amide on the surface. Formation of the amide bond and the presence of the attached functional moiety are monitored with polarization modulation Fourier transform infrared (PM-FTIR) vibrational spectroscopy.<sup>5</sup> Additional X-ray photoelectron spectroscopy (XPS) measurements are used to estimate the relative surface coverage of the attached species. The acid chloride intermediate can also react with alcohols to form an ester linkage, and the attachment of an electrochemically active ferrocene species to the gold surface with an ester formation reaction is demonstrated. The surface coverage of the attached ferrocene species is determined with electrochemical measurements.

### EXPERIMENTAL SECTION

**Molecules.** 11-Mercaptoundecanoic acid ( $\text{HSC}_{10}\text{H}_{20}\text{COOH}$ ) was obtained from Aldrich, and the purity was checked by NMR spectroscopy. The octadecanethiol ( $\text{HSC}_{18}\text{H}_{37}$ ) used in comparison experiments was obtained from Fluka (~95%) and used as received. Methylene chloride (HPLC grade) was obtained from Burdick & Jackson and used as received except for the esterification reaction where it was purified by distillation (mainly to remove water). Hexylamine (~99%, Fluka) and benzylamine (99%, Aldrich) were used without further purification. Aniline (>99.5%, Aldrich) was used immediately after distillation at reduced pressure in a fume hood. Care must be taken to avoid contact with aniline since it is highly toxic. Decomposition of the aniline was avoided by limiting its exposure to light and oxygen. Thionyl chloride (99+%, Aldrich) was used as received. Thionyl chloride should be used in a fume hood and kept under nitrogen at all times since it is toxic and readily hydrolyzed in air. The phosphate buffer was prepared from  $\text{NaNO}_3$  (>99.5%, Fluka),  $\text{Na}_2\text{HPO}_4$  (>99.0%, Fluka), and ortho- $\text{H}_3\text{PO}_4$  (puriss, Fluka) reagents which were used as received. Distilled, deionized

water was obtained from a Millipore system and then further purified through double-distillation.

**Electrode Preparation.** Gold foils (99.9+%, D. F. Goldsmith) 0.010 in. thick were used as a substrate. Prior to deposition the gold surface was polished to a mirror finish with 0.05- $\mu\text{m}$  alumina particles, rinsed thoroughly with triply-distilled water, and sonicated for approximately 15 min in triply-distilled water. The polished substrates were then cleaned by a standard sulfuric acid (concentrated)/hydrogen peroxide (30%) cleaning procedure for 15 min.<sup>7</sup> Precautions should be taken to avoid contact with this highly oxidizing mixture which should be prepared immediately before use. This mixture should be discarded immediately after use since it may be explosive if stored.<sup>8</sup> Upon removal from the sulfuric acid/hydrogen peroxide bath, the Au foils were rinsed with triply-distilled water and dried with a stream of dry nitrogen in an ambient laboratory environment before use in the spontaneous adsorption process.

**FTIR Measurements.** Infrared differential reflectance spectra ( $-\% \Delta R/R$ ) were obtained with a Nicolet 740 spectrometer that had been modified to perform dual-channel polarization modulation Fourier transform infrared (PM-FTIR) spectroscopic experiments.<sup>9,10</sup> The differential reflectance spectra are expressed as  $(-\% \Delta R/R) = 100(R_s - R_p)/(R_p + R_s)$  where  $R_p$  and  $R_s$  are the reflectivity for p- and s-polarized light from the surface. Spectra were obtained at a nominal resolution of 2  $\text{cm}^{-1}$ . The angle of incidence for the differential reflectance measurements was 76° from the surface normal. No reference sample for a background was required with the PM-FTIR measurements. Instead, the spectra were normalized for variations with wavelength in the efficiency of the photoelastic modulator as described previously.<sup>11</sup> Full descriptions of the experimental apparatus and the PM-FTIR methodology are described elsewhere.<sup>6,9,11</sup>

**XPS Measurements.** The XPS spectra were obtained with a Perkin-Elmer 5400 ESCA photoelectron spectrometer with an achromatic Mg K $\alpha$  source ( $E = 1253.6$  eV, 300 W) operating in the fixed analyzer transmission mode. The scan area was 1  $\times$  3 mm in which the gold-foil surface normal was at 45° to the entrance of the concentric hemispherical analyzer. The XPS measurements were made at a base pressure of about 10<sup>-9</sup> Torr. Multiplex spectra of the individual elements were performed using a 35.75 eV pass energy. No charging effects were observed in the emission spectrum, as evidenced by the position of the C 1s peak at 285.0 eV.<sup>12</sup> Relative intensities are obtained from ratios of integrated peak areas and then normalized by the appropriate instrumental sensitivity factors.<sup>12</sup>

**Electrochemical Measurements.** The derivatized ferrocene electrode was characterized by its cyclic voltammogram (CV) in an aqueous solution of 0.05 M phosphate buffer with 0.2 M NaNO<sub>3</sub> supporting electrolyte at pH = 7.1 under nitrogen at 298 K. A single-compartment Teflon cell (solution volume  $\approx$  10 mL) employing a standard three-electrode arrangement (Pt counter electrode, saturated calomel (SCE) reference electrode) was used in conjunction with an IBM EC 225 potentiostat interfaced to an IBM-XT computer.

## RESULTS AND DISCUSSION

**Carboxylic Acid Monolayer Adsorption.** Molecules of HSC<sub>10</sub>H<sub>20</sub>COOH were adsorbed onto a polycrystalline gold surface by immersion for approximately 1 h in a 2 mM solution in methylene chloride. Immersion of the surface for a longer period (up to 2 days) resulted in no observable spectroscopic differences. After thoroughly rinsing with methylene chloride, the infrared differential reflectance spectrum of the monolayer was obtained with PM-FTIR spectroscopy: the CH-stretching region and the mid-IR region of this spectrum are plotted in Figures 1 and 2a; respectively. Monolayers of this molecule have been formed previously on gold surfaces by Chidsey and Loiacono;<sup>13</sup> monolayers of the similar molecule HSC<sub>16</sub>H<sub>32</sub>COOH have been studied in detail by Nuzzo et al.<sup>14</sup> As noted by Chidsey and Loiacono,<sup>13</sup> the frequencies of the two methylene stretching bands at 2924 and 2856  $\text{cm}^{-1}$  in Figure 1 suggest that the alkyl chains of the C<sub>10</sub> carboxylic acid monolayer are more disorganized than those in the C<sub>16</sub> analogue.<sup>15</sup> The "liquidlike" structure that occurs in these car-

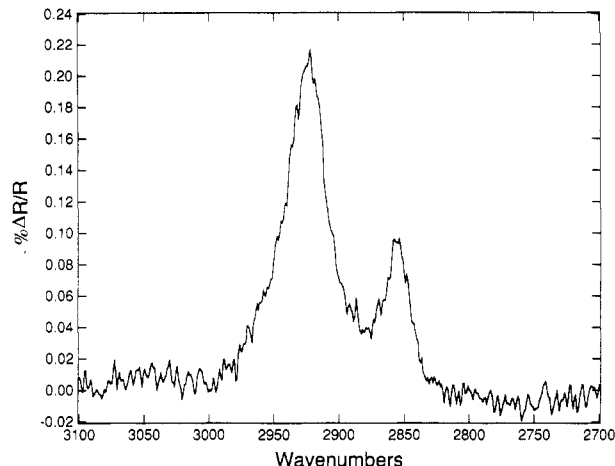


**Figure 1.** PM-FTIR differential reflectance spectrum of the CH-stretching region from a spontaneously organized monolayer of 11-mercaptoundecanoic acid adsorbed onto a polycrystalline gold substrate. The antisymmetric methylene-stretching band at 2924  $\text{cm}^{-1}$  indicates a disordered, liquidlike structure. The symmetric methylene-stretching band is at 2856  $\text{cm}^{-1}$ .

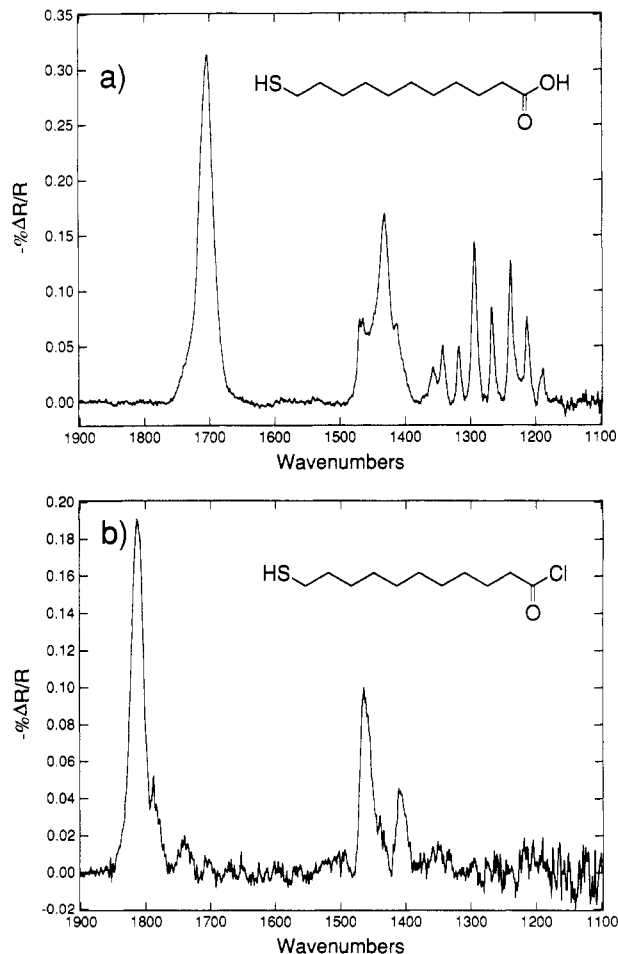


**Figure 2.** The mid-IR region differential reflectance spectrum from a spontaneously organized monolayer of (a) 11-mercaptoundecanoic acid adsorbed onto a polycrystalline gold substrate and (b) the acid chloride derivative of the 11-mercaptoundecanoic acid monolayer in (a) after modification by the gas-phase reaction with thionyl chloride.

boxylic acid monolayers was not observed in the well-ordered alkane or alcohol monolayers of the same length.<sup>13</sup> For the experiments reported in this paper, the C<sub>10</sub> carboxylic acid monolayer with its conformational disorder was chosen in order to permit the acid head group to have sufficient freedom to react in a sterically unhindered fashion but still to have

**Table I. XPS Measurements of Relative Elemental Surface Coverage for the Adsorbed Monolayers**

| compd   | element            | binding energies, <sup>a</sup><br>eV | rel intens <sup>b</sup> |
|---|--------------------|--------------------------------------|-------------------------|
| octadecanethiol<br>(HSC <sub>18</sub> H <sub>37</sub> )                               | S                  | 162.3                                | 1.00                    |
| 11-mercaptoundecanoic acid<br>(HSC <sub>10</sub> H <sub>20</sub> COOH)                | S                  | 162.3                                | 0.88 ± 0.05             |
|   | C <sub>alkyl</sub> | 285.0                                | 11.38 ± 0.34            |
|   | C <sub>acid</sub>  | 289.0                                | 1.03 ± 0.09             |
| hexylamide<br>(HSC <sub>10</sub> H <sub>20</sub> CONHC <sub>6</sub> H <sub>13</sub> ) | O                  | 532.5                                | 1.68 ± 0.06             |
|   | S                  | 162.3                                | 0.99 ± 0.05             |
|   | N                  | 400.2                                | 0.88 ± 0.05             |
| benzylamide<br>(HSC <sub>10</sub> H <sub>20</sub> CONHCH <sub>2</sub> φ)              | O                  | 532.2                                | 0.91 ± 0.03             |
|   | N                  | 400.3                                | 0.83 ± 0.05             |
|   | S                  | 162.3                                | 0.91 ± 0.05             |
| aniline amide<br>(HSC <sub>10</sub> H <sub>20</sub> CONHφ)                            | O                  | 532.2                                | 0.88 ± 0.03             |
|   | N                  | 400.0                                | 0.76 ± 0.05             |
|   | S                  | 162.3                                | 0.96 ± 0.05             |
| ferrocene ester<br>(HSC <sub>10</sub> H <sub>20</sub> COOCH <sub>2</sub> Fc)          | Fe <sup>c</sup>    | 708.1                                | 0.27 ± 0.02             |
|   | O                  | 532.2                                | 1.71 ± 0.06             |
|   | S                  | 162.3                                | 0.87 ± 0.04             |

<sup>a</sup> Referenced to C 1s at 285.0 eV.<sup>12</sup> <sup>b</sup> Normalized to the S 2p intensity of octadecanethiol. Intensities were measured as the integrated peak areas. <sup>c</sup> The relative amount of ferrocene ester was determined using the Fe 2p<sub>3/2</sub> response.

enough interaction energy between the chains to ensure that the molecules were strongly adsorbed. Further evidence for the flexibility of the head group is seen in the C=O-stretching band in Figure 2a. The observed frequency of 1704 cm<sup>-1</sup> is that expected for acid groups that are participating in dimerization or other intermolecular hydrogen-bonding processes.<sup>14,16</sup> For comparison, the C=O-stretching band in the C<sub>16</sub> monolayer, where the head group cannot interact, occurs at 1741 cm<sup>-1</sup>.<sup>14</sup>

In addition to the C=O stretch, the mid-IR spectrum in Figure 2a also contains bands due to the CH<sub>2</sub> scissors deformation (1470 cm<sup>-1</sup>) and the CH rocking and wagging motions (≈1350–1150 cm<sup>-1</sup>) of the adsorbed molecules (cf. Table II). The significant intensities of these bands in the C<sub>11</sub> monolayer suggest that the alkyl chains are orientationally disordered with respect to the surface.<sup>17</sup> This orientational disorder can be attributed to both the flexibility of the short alkyl chain and the microscopic roughening that is inevitable on the polished polycrystalline gold surfaces. However, the

definite progressions in the wagging and rocking bands indicate that although the alkyl chains are orientationally disordered, the conformational order is much higher than that observed in the liquid state.<sup>18</sup>

In addition to the PM-FTIR measurements, XPS experiments were used to verify the presence of sulfur and carboxylic acid moieties on the surface. The C 1s XPS spectrum exhibited a peak at 289.1 eV that has been attributed previously to the carboxylic acid carbon.<sup>19</sup> The thiolate sulfur on the surface was monitored via the intensity of the S 2p peak at 162.3 eV. Overexposure (anode power > 300 W) of the surface resulted in the appearance of an additional S 2p peak at ca. 169 eV, as noted previously by other authors.<sup>14</sup> For all of the monolayers studied the intensity of this peak was constant to within ±10–15% and was roughly the same as that observed from a packed monolayer of a C<sub>18</sub> alkanethiol (HSC<sub>18</sub>H<sub>37</sub>). This result in conjunction with the observed intensity of the CH-stretching band confirms that throughout the course of the surface reactions, the surface coverage remained at about one monolayer (±20%). The XPS results are tabulated in Table I.

**Acid Chloride Formation Reaction.** In order to activate the alkanethiol monolayer, the carboxylic acid was converted to an acid chloride by reaction with thionyl chloride in a gas-phase reaction under reduced pressure. Samples were placed in a reaction vessel that was back-filled with N<sub>2</sub> and evacuated to approximately 300–500 mTorr. The reaction vessel consisted of a standard three-necked 250-mL round-bottom flask that could be connected to either a vacuum system or a dry nitrogen supply.<sup>20</sup> A 25-μL aliquot of SOCl<sub>2</sub> was then injected into the reaction vessel and allowed to react for 5–10 min. The vessel was then pumped down to 300–500 mTorr to remove any HCl and other reaction byproducts for 15–30 min. Efforts to make this reaction proceed in a chloroform solution led to a loss of the monolayer from the surface (as verified by PM-FTIR measurements), and subsequent rinsing of the sample in methylene chloride also resulted in the removal of the acid chloride. If the monolayer was prevented from coming in contact with atmospheric water, the PM-FTIR spectrum of the acid chloride monolayer could be obtained (Figure 2b). In this spectrum, the C=O-stretching band has shifted to 1813 cm<sup>-1</sup>, as expected for an acid chloride species.<sup>21</sup> Exposure to atmospheric water slowly reconverted the acid chloride to the acid, first developing a band at 1741 cm<sup>-1</sup> (the isolated acid species observed in the C<sub>16</sub> monolayers)

**Table II. Infrared Frequencies and Vibrational Assignments for the Derivatized Monolayers in the Mid-IR Region<sup>a</sup>**

| derivatized monolayer film  | frequency, cm <sup>-1</sup> <sup>b</sup> | assgnt <sup>c</sup>                  |  |
|---|--|--------------------------------------|--|
| 11-mercaptoundecanoic acid<br>(HSC <sub>10</sub> H <sub>20</sub> COOH)                | 1704                                     | ν <sub>C=O</sub> (CO <sub>2</sub> H) | carboxylic acid C=O stretch<br>C—O stretch <sup>d</sup> (+ ip COH bend)<br>acid chloride C=O stretch <sup>30</sup>   |
|   | 1431                                     | ν <sub>C—O</sub>                     |  |
|   | 1813                                     | ν <sub>C=O</sub> (COCl)              |  |
| hexylamide<br>(HSC <sub>10</sub> H <sub>20</sub> CONHC <sub>6</sub> H <sub>13</sub> ) | 1660                                     | ν <sub>C=O</sub>                     | amide I<br>amide II<br>amide I<br>amide II<br>φ ring str vibr <sup>22</sup><br>φ ring str vibr <sup>22</sup>   |
|   | 1550                                     | ν <sub>O=C—N—H</sub>                 |  |
|   | 1642                                     | ν <sub>C=O</sub>                     |  |
|   | 1552                                     | ν <sub>O=C—N—H</sub>                 |  |
|   | 1604                                     | ν <sub>C=C</sub>                     |  |
|   | 1500                                     | ν <sub>C=C</sub>                     |  |
| benzylamide<br>(HSC <sub>10</sub> H <sub>20</sub> CONHCH <sub>2</sub> φ)              | 1655                                     | ν <sub>C=O</sub>                     | amide I<br>amide II<br>φ ring str vibr <sup>22</sup><br>φ ring str vibr <sup>22</sup><br>φ ring str vibr <sup>22</sup>   |
|   | 1550                                     | ν <sub>O=C—N—H</sub>                 |  |
|   | 1604                                     | ν <sub>C=C</sub>                     |  |
|   | 1500                                     | ν <sub>C=C</sub>                     |  |
|   | 1731                                     | ν <sub>C=O</sub> (CO <sub>2</sub> R) |  |
| aniline amide<br>(HSC <sub>10</sub> H <sub>20</sub> CONHφ)                            | 1411                                     | ν <sub>C=C</sub>                     | ester C=O stretch<br>(E <sub>1u</sub> ) Cp ring str vibr <sup>25,27</sup><br>ester C—O stretch <sup>26</sup><br>(A <sub>2u</sub> ) Cp ring str vibr <sup>25,27</sup> |
|   | 1237                                     | ν <sub>C—O</sub>                     |  |
|   | 1105                                     | ν <sub>C=C</sub>                     |  |
|   | 1105                                     | ν <sub>C=C</sub>                     |  |

<sup>a</sup> Only the amide bands, ester bands, and bands characteristic of the attached pendant functional groups are listed. <sup>b</sup> Band positions were obtained from the 2-cm<sup>-1</sup> resolution spectra shown in Figure 3. <sup>c</sup> Assignments were taken from refs 14 or 23 unless otherwise noted. <sup>d</sup> This mode may also contain substantial C—O—H bending character.<sup>14,16a,22</sup>

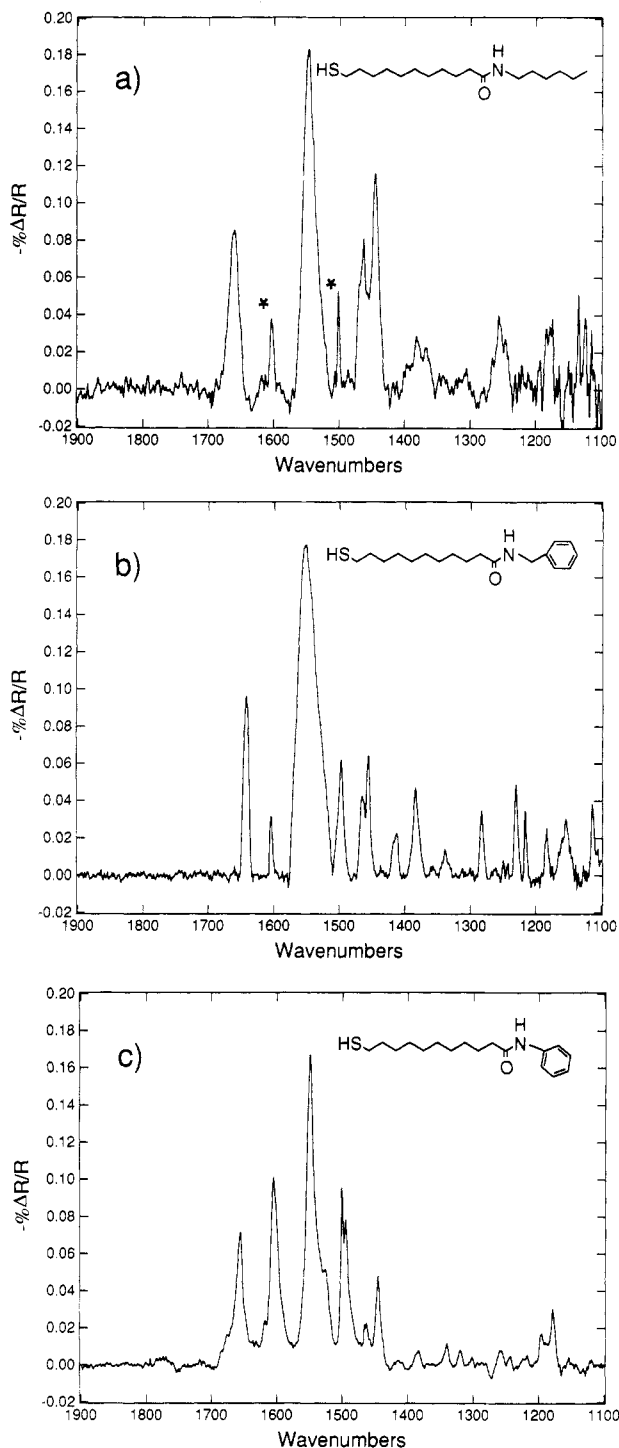


**Figure 3.** PM-FTIR differential reflectance spectrum from the amide monolayers formed by the surface reaction of 11-mercaptoundecanoic acid and the amine  $\text{RNH}_2$  is (a) *n*-hexylamine (where asterisks denote aromatic impurity bands), (b) benzylamine, (c) aniline.

that was slowly replaced by the original band at  $1704\text{ cm}^{-1}$ .

**Amide Derivatization Reactions.** Following the formation of the acid chloride, the alkanethiol monolayer could be converted to an amide by the introduction of an amine into the gas phase of the reaction vessel. Removal of any unreacted amine was accomplished by first purging the reaction chamber and then by rinsing the surface with various solvents (the exact solvent used depended upon the nature of the attached species). Three different amines were attached to the surface via an amide formation reaction: *n*-hexylamine, benzylamine, and aniline. The PM-FTIR spectra of the amides formed on the surface from these three compounds are shown in Figure

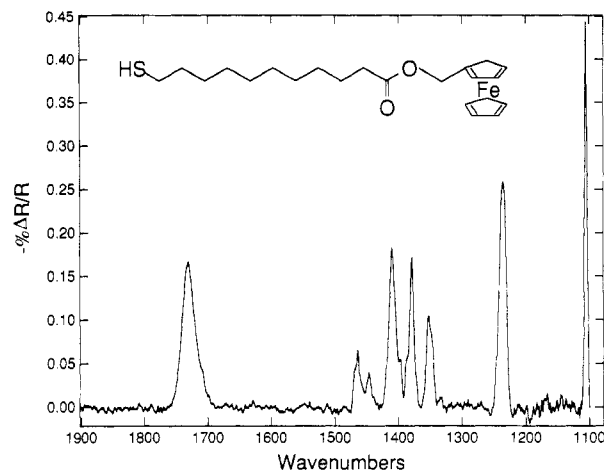


**Figure 4.** PM-FTIR differential reflectance spectrum from the ferrocene monolayer formed by the surface reaction of 11-mercaptoundecanoic acid and (hydroxymethyl)ferrocene.

3. All of the amines exhibit the characteristic amide I and II bands at  $1642\text{--}60$  and  $1550\text{ cm}^{-1}$ ,<sup>22-24</sup> as well as additional bands due to the rest of the attached molecule. Table II summarizes the mid-IR vibrational assignments of these derivatized monolayers. The broad, asymmetric shape of the amide I and II bands indicates a distribution of hydrogen-bonded species.<sup>14,22</sup> The reaction with benzylamine demonstrates that large groups can be attached to the surface (as expected from the high degree of conformational disorder of the monolayer), and the reaction with aniline demonstrates that both aromatic as well as aliphatic amines can be employed. The sensitivity of the PM-FTIR measurements is demonstrated by the presence of two bands due to the aromatic amine impurities in the hexylamide spectra (denoted by the asterisks in Figure 3a).

Further confirmation of the surface amide formation was obtained with XPS spectroscopy. A N 1s peak was observed at  $400.3\text{ eV}$  for the three amide-derivatized monolayers (no N 1s peak was observed for the carboxylic acid film). A relative intensity of ca. 0.9 for this peak compared to the S 2p peak intensity was calculated for each sample, using previously determined instrumental sensitivity factors (cf. Table I). Since the sulfur peak intensity is undoubtedly diminished relative to the N peak due to screening by the alkyl chain, this number must be used as an upper limit for the N/S ratio on the surface. In addition, a decrease by approximately a factor of 2 in the relative intensity of the O 1s peak was observed after reaction of the 11-mercaptoundecanoic acid to form the amide.

**Ferrocene Ester Derivatization Reaction.** In addition to the formation of an amide bond, the surface acid chloride could be easily converted to an ester by reaction with an alcohol. For example, the reaction of a monolayer of acid chloride species with ethanol resulted in the quantitative formation of a monolayer of the ethyl ester,  $\text{HSC}_{10}\text{H}_{20}\text{COOC}_2\text{H}_5$ . Similarly, the ester formation reaction with (hydroxymethyl)ferrocene ( $\text{FcCH}_2\text{OH}$ ) produced a gold surface with a chemically-attached monolayer ( $\text{HSC}_{10}\text{H}_{20}\text{COOCH}_2\text{Fc}$ ) which was electrochemically active. For this reaction, (hydroxymethyl)ferrocene was introduced into the reaction vessel via atomization of a  $0.3\text{ M}$  methylene chloride solution of the alcohol at a reduced pressure of  $300\text{--}500\text{ mTorr}$ . The PM-FTIR spectrum of the ferrocene monolayer is shown in Figure 4 and contains ester stretches at  $1731$  and  $1237\text{ cm}^{-1}$  as well as the characteristic ferrocene ring stretch at  $1105\text{ cm}^{-1}$ .<sup>25-27</sup> Prior to rinsing, a residual acid chloride band at  $1813\text{ cm}^{-1}$  was observed, indicating incomplete ester formation on the surface. XPS measurements of the Fe  $2p_{3/2}$  peak at  $708.1\text{ eV}$ <sup>28</sup>

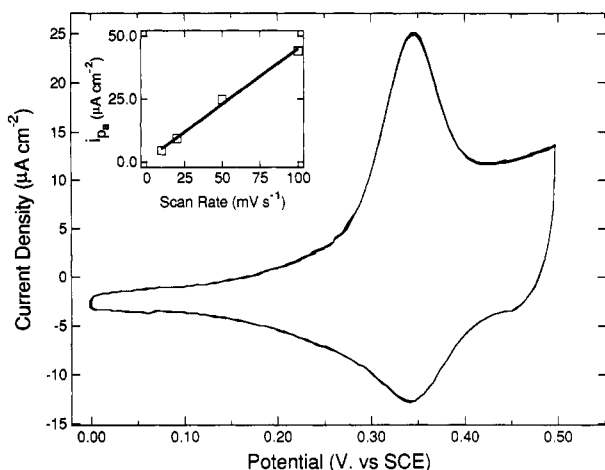


**Figure 5.** CV of the partial monolayer of the derivatized ferrocene ester in 0.05 M phosphate buffer with 0.2 M  $\text{NaNO}_3$  supporting electrolyte adjusted with phosphoric acid to  $\text{pH} = 7.1$ . The sweep rate was  $50 \text{ mV s}^{-1}$ . Integration of the anodic current peak yielded a surface charge density of  $23.2 \mu\text{C cm}^{-2}$ . The figure insert plots the anodic peak current density,  $i_{p_a}$ , at 0.34 V vs SCE which varies linearly as a function of scan rate.

confirmed the presence of the ferrocene group on the surface in submonolayer quantities (see Table I). The incomplete reaction of (hydroxymethyl)ferrocene with the acid chloride as compared to the ethanol reaction can be attributed to both the lower vapor pressure of the ferrocene species and possible steric hindrance effects resulting from the size of the ferrocene head group.

Following rinsing with methylene chloride and triply-distilled water, a CV was obtained from this modified electrode surface in a  $\text{pH} = 7.1$  phosphate buffer (Figure 5). Plotted in the inset of the figure is the anodic peak current density as a function of scan rate, which exhibited a linear dependence as expected for a surface species. Integration of this ferrocene oxidation peak yielded a surface charge density of  $23.2 \mu\text{C cm}^{-2}$ , corresponding to a surface coverage of  $2.4 \times 10^{-10} \text{ mol cm}^{-2}$ . This number corresponds to approximately 40% of a monolayer of close-packed ferrocene molecules.<sup>29</sup> The actual surface coverage varied from film to film by ca. 20%.

The reduction peak for the ferrocenium occurred at approximately the same potential (to within 5–30 mV) of the ferrocene oxidation peak, as expected for a surface electroactive species. However, the return peak is much broader and asymmetric due to a combination of capacitance and film reorganization effects. (Note that although it appears as if the integrated charge of the ferrocenium reduction peak is smaller than that of the ferrocene oxidation peak, the integrated area of the two peaks are approximately the same.) The form of this CV was stable for several hours. Further studies of these reorganization effects are in progress.

## CONCLUSIONS

This paper presents the experimental verification of a general scheme for the modification of monolayers at gold surfaces utilizing gas-phase surface reactions. The bifunctional molecule (11-mercaptoundecanoic acid) attaches to gold surfaces via the thiol group, and provides a carboxylic acid functionality that can be converted to an acid chloride by reaction in the gas phase with thionyl chloride. The resultant acid chloride intermediate could then be further reacted in the gas phase with either an amine for the formation of an amide or an alcohol to form an ester. Three different amines (hexylamine, benzylamine, and aniline) and an electroactive alcohol (hydroxymethyl)ferrocene were attached to a polycrystalline gold surface to demonstrate the versatility of this methodology.

Verification of the surface reactions was achieved through the use of PM-FTIR spectroscopy, which demonstrated submonolayer sensitivity to the presence of the carboxylic acid, amide and ester species on the surface. The PM-FTIR differential reflectance spectra were also used to spectroscopically identify the pendant groups attached to the monolayers. XPS and electrochemical measurements were performed in conjunction with vibrational spectroscopy to confirm the PM-FTIR results.

In the future, this general attachment scheme should serve as a valuable route to the synthesis of many optically and electrochemically interesting monolayers at gold surfaces. Further experiments on the modified monolayers presented in this paper are currently in progress.

## ACKNOWLEDGMENT

We thank Matthew J. Smith of Nicolet Instrument Corp. for his assistance in implementing the dual-channel PM-FTIR experiment. Financial support from the National Science Foundation is gratefully acknowledged.

**Registry No.**  $\text{HSC}_{10}\text{H}_{20}\text{COOH}$ , 71310-21-9;  $\text{HSC}_{10}\text{H}_{20}\text{COCl}$ , 54654-13-6;  $\text{HSC}_{10}\text{H}_{20}\text{CONHC}_6\text{H}_{13}$ , 138153-90-9;  $\text{HSC}_{10}\text{H}_{20}\text{CONHCH}_2\text{O}$ , 138153-91-0;  $\text{HSC}_{10}\text{H}_{20}\text{CONHO}$ , 138153-92-1;  $\text{HSC}_{10}\text{H}_{20}\text{COOC}_2\text{H}_5$ , 1725-06-0;  $\text{HSC}_{18}\text{H}_{37}$ , 2885-00-9;  $\text{C}_6\text{H}_{13}\text{NH}_2$ , 111-26-2;  $\text{OCH}_2\text{NH}_2$ , 100-46-9;  $\text{ONH}_2$ , 62-53-3;  $\text{SOCl}_2$ , 7719-09-7;  $\text{H}_2\text{O}_2$ , 7722-84-1;  $\text{NaNO}_3$ , 7631-99-4;  $\text{CH}_2\text{Cl}_2$ , 75-09-2; Au, 7440-57-5;  $\text{C}_2\text{H}_5\text{OH}$ , 64-17-5;  $\text{HOCH}_2\text{Fc}$ , 1273-86-5;  $\text{HSC}_{10}\text{H}_{20}\text{COOCH}_2\text{Fc}$ , 138180-87-7.

## REFERENCES

- (1) (a) Swalen, J. D.; Allara, D. L.; Andrade, J. D.; Chandross, E. A.; Garoff, S.; Israelachvili, J.; McCarthy, T. J.; Murray, R. W.; Pease, R. F.; Rabolt, J. F.; Wynne, K. J.; Yu, H. *Langmuir* **1987**, *3*, 932–950. (b) Adamson, A. W. *Physical Chemistry of Surfaces*; Wiley: New York, 1990. (c) Bregman, J. I. *Corrosion Inhibitors*; MacMillan: New York, 1963; Chapter 5. (d) Bowden, F. P.; Tabor, D. *The Friction and Lubrication of Solids*; Oxford University Press: London, 1968; Part II, Chapter 19. (e) Zisman, W. A. *In Friction and Wear*; Davis, R., Ed.; Elsevier: New York, 1959. (f) Gaines, G. L., Jr. *Immiscible Monolayers at the Liquid-Gas Interfaces*; Wiley: New York, 1966.
- (2) (a) Allara, D. L.; Swalen, J. D. *J. Phys. Chem.* **1982**, *86*, 2700–2704. (b) Gun, J.; Iscovici, R.; Sagiv, J. *J. Colloid Sci.* **1984**, *101*, 201–213. (c) Moaz, R.; Sagiv, J. *J. Colloid Sci.* **1984**, *100*, 485–495. (d) Moaz, R.; Sagiv, J. *Langmuir* **1987**, *3*, 1034–1044. (e) Moaz, R.; Sagiv, J. *Langmuir* **1987**, *3*, 1045–1051.
- (3) (a) Porter, M. D.; Bright, T. B.; Allara, D. L.; Chidsey, C. E. D. *J. Am. Chem. Soc.* **1987**, *109*, 3559–3568. (b) Nordyke, L. L.; Buttry, D. A. *Langmuir* **1991**, *7*, 380–386. (c) Chidsey, C. E. D. *Science* **1991**, *251*, 919–922. (d) Nuzzo, R. G.; Fusco, F. A.; Allara, D. L. *J. Am. Chem. Soc.* **1987**, *109*, 2358–2368. (e) Bain, C. D.; Whitesides, G. M. *J. Am. Chem. Soc.* **1988**, *110*, 3665–3666. (f) Stole, S. M.; Porter, M. D. *Langmuir* **1990**, *6*, 1199–1202. (g) Strong, L.; Whitesides, G. M. *Langmuir* **1988**, *4*, 546–558.
- (4) (a) Creager, S. E.; Collard, D. M.; Fox, M. A. *Langmuir* **1990**, *6*, 1617–1620. (b) Putviniski, T. M.; Schilling, M. L.; Katz, H. E.; Chidsey, C. E. D.; Mujisce, A. M.; Emerson, A. B. *Langmuir* **1990**, *6*, 1567–1571. (c) Dubois, L. H.; Zegarski, B. R.; Nuzzo, R. G. *J. Am. Chem. Soc.* **1990**, *112*, 570–579. (d) Tillman, N.; Ullman, A.; Penner, T. L. *Langmuir* **1989**, *5*, 101–111.
- (5) (a) Murray, R. W. *In Electroanalytical Chemistry*; Bard, A. J., Ed.; Marcel Dekker: New York, 1984; Vol. 13, pp 191–368 and references therein. (b) Abruna, H. D.; Meyer, T. J.; Murray, R. W. *Inorg. Chem.* **1979**, *18*, 3233–3240.
- (6) (a) Golden, W. G. *Fourier Transform Infrared Spectroscopy*, **1985**, *4*, 315. (b) Golden, W. G.; Saperstein, D. D.; Severson, M. W.; Overend, J. *J. Phys. Chem.* **1984**, *88*, 574–580. (c) Dowrey, A. E.; Marcott, C. *Appl. Spectrosc.* **1982**, *36*, 414–416. (d) Nafie, L. A. *In Applied Fourier Transform Infrared Spectroscopy*; Mackenzie, M. W., Ed.; Wiley: New York, 1988. (e) Golden, W. G.; Kunimatsu, K.; Seki, H. *J. Phys. Chem.* **1984**, *88*, 1275–1277. (f) Kunimatsu, K.; Golden, W. G.; Seki, H.; Philippot, M. R. *Langmuir* **1985**, *1*, 245–250.
- (7) Finklea, H. O.; Robinson, L. R.; Blackburn, A.; Richter, B.; Allara, D.; Bright, T. *Langmuir* **1988**, *2*, 239–244.
- (8) Dobbs, D. A.; Bergman, R. G.; Theopold, K. H. *Chem. Eng. News*, **1990**, *68* (17), 2.
- (9) Green, M. J.; Barner, B. J.; Corn, R. M. *Rev. Sci. Instrum.* **1991**, *62*, 1426–1430.
- (10) Buffeteau, T.; Desbat, B.; Turlot, J. M. *Mikrochim. Acta* **1988**, *2*, 23.
- (11) Barner, B. J.; Green, M. J.; Saez, E. I.; Corn, R. M. *Anal. Chem.* **1991**, *63*, 55–60.
- (12) Briggs, D.; Seah, M. P., Eds. *Practical Surface Analysis by Auger and X-ray Photoelectron Spectroscopy*; Wiley: New York, 1983.
- (13) Chidsey, C. E. D.; Lolocono, D. N. *Langmuir* **1990**, *6*, 682–691.
- (14) Nuzzo, R. G.; Dubois, L. H.; Allara, D. L. *J. Am. Chem. Soc.* **1990**, *112*, 558–569.

- (15) Snyder, R. G.; Strauss, H. L.; Elliger, C. A. *J. Phys. Chem.* **1982**, *86*, 5145-5150.
- (16) (a) Umemura, J. *J. Chem. Phys.* **1978**, *68*, 42-48. (b) Kishida, S.; Nakamoto, K. *J. Chem. Phys.* **1964**, *41*, 1558-1563. (c) Krause, P. F.; Katon, J. E.; Rogers, J. M.; Phillips, D. B. *Appl. Spectrosc.* **1977**, *31*, 110-115.
- (17) Snyder, R. G.; Schachtschneider, J. H. *Spectrochim. Acta* **1963**, *19*, 85-116.
- (18) Snyder, R. G.; Marconelli, M.; Strauss, H. L.; Hallmark, V. M. *J. Phys. Chem.* **1986**, *90*, 5623-5630.
- (19) Troughton, E. B.; Bain, C. D.; Whitesides, G. M.; Nuzzo, R. G.; Allara, D. L.; Porter, M. D. *Langmuir* **1988**, *4*, 365-385.
- (20) Duevel, R. V. Ph.D. Thesis, University of Wisconsin at Madison, 1991.
- (21) (a) Overend, J.; Scherer, J. R. *Spectrochim. Acta* **1960**, *16*, 773-782. (b) Kagarise, R. E. *J. Am. Chem. Soc.* **1955**, *77*, 1377-1379. (c) Bellamy, L. J.; Williams, R. L. *J. Chem. Soc.*, **1958**, 3465-3468.
- (22) Bellamy, L. J. *The Infrared Spectra of Complex Molecules*; Wiley: New York, 1975.
- (23) (a) Miyazawa, T.; Shimanouchi, T.; Mizushima, S.-I. *J. Chem. Phys.* **1958**, *29*, 611-616. (b) Tornkvist, C.; Liedberg, B.; Lundstrom, I. *Langmuir* **1991**, *7*, 479-485.
- (24) Suzuki, I. *Bull. Chem. Soc. Jpn.* **1962**, *35*, 1279-1286.
- (25) Lippincott, E. R.; Nelson, R. D. *Spectrochim. Acta* **1958**, *10*, 307-329.
- (26) Wilmshurst, J. K. *J. Mol. Spectrosc.* **1957**, *1*, 201-215.
- (27) Maslowsky, E., Jr. *J. Mol. Struct.* **1974**, *21*, 464-468.
- (28) Lenhard, J. R.; Murray, R. W. *J. Am. Chem. Soc.* **1978**, *100*, 7870-7875.
- (29) Chidsey, C. E. D.; Bertozzi, C. R.; Putvinski, T. M.; Mujsc, A. M. *J. Am. Chem. Soc.* **1990**, *112*, 4301-4306.
- (30) Bain, C. D.; Biebuyck, H. A.; Whitesides, G. M. *Langmuir* **1989**, *5*, 723-727.

RECEIVED for review September 17, 1991. Accepted November 15, 1991.

## Enzymatically Amplified Time-Resolved Fluorescence Immunoassay with Terbium Chelates

Theodore K. Christopoulos and Eleftherios P. Diamandis\*

Department of Clinical Biochemistry, Toronto Western Hospital, 399 Bathurst Street, Toronto, Ontario M5T 2S8, Canada, and Department of Clinical Biochemistry, University of Toronto, 100 College Street, Toronto, Ontario M5G 1L5, Canada

**We report an ultrasensitive, enzymatically amplified, time-resolved fluorescence immunoassay with a terbium chelate as the detectable moiety. In this immunoassay, the primary label is the enzyme alkaline phosphatase (ALP). ALP cleaves phosphate out of a fluorogenic substrate, 5-fluorosallycyl phosphate, to produce 5-fluorosallyclic acid (FSA). 5-Fluorosallyclic acid can then form a highly fluorescent ternary complex of the form FSA-Tb<sup>3+</sup>-EDTA, which can be quantified by measuring the Tb<sup>3+</sup> fluorescence in a time-resolved mode. In this assay, exceptional sensitivity is achieved because of the enzymatic amplification introduced by ALP and the quantification by laser-induced microsecond time-resolved fluorometry. Time-resolved fluorometry is applicable because of the long fluorescence lifetime of the Tb<sup>3+</sup> complexes. It is shown that in a model AFP assay 10<sup>6</sup> or 1.5 × 10<sup>5</sup> molecules can be detected (final assay volume, 100 μL) by using monoclonal or polyclonal detection antibodies, respectively. The assay demonstrates excellent precision (~4%), and it seems to be highly suited for automated, sensitive, and rapid immunoassays.**

### INTRODUCTION

Among the nonisotopic immunoassay methodologies, time-resolved fluorescence immunoassay is well-established and successful. The commercially available systems are based on the use of fluorescent europium chelates as labels, and the technology has been recently reviewed.<sup>1-5</sup> The main advantages of the fluorescent europium chelates have been repeatedly stressed. These are also shared with other lanthanide chelates and especially with the fluorescent Tb<sup>3+</sup> and Sm<sup>3+</sup> chelates. Such advantages include large Stokes shifts, narrow

emission bands, and long fluorescence lifetimes. The long lifetime makes these chelates especially suitable as labels for microsecond time-resolved fluorescence immunoassay.

Europium has been, up to now, the lanthanide label of choice for time-resolved fluorescence immunoassay because of its superior detectability in comparison to Tb<sup>3+</sup> and more so to Sm<sup>3+</sup>.<sup>6</sup> The last two lanthanides have primarily been used as comparison labels to devise dual analyte assays as described elsewhere.<sup>7-10</sup> Tb<sup>3+</sup> alone has been proposed as a primary immunological or nucleic acid label mainly because of its ability to form ternary fluorescent mixed complexes with aminopolycarboxylic acids (e.g. EDTA or DTPA) and certain ligands like *p*-aminosalicylate.<sup>11-15</sup> However, the better sensitivity of the Eu<sup>3+</sup>-assayed systems precluded the widespread use of these complexes.

Tb<sup>3+</sup> complexes, however, have some advantages over the Eu<sup>3+</sup> complexes. Tb<sup>3+</sup> can form fluorescent complexes with a wider variety of organic ligands, many of these complexes are freely soluble in water, and quenching by coordinated water molecules is not a serious problem. On the other hand, in ternary Tb<sup>3+</sup> complexes, slight modification of the coordinated ligand, especially on the hydroxyl which is adjacent to the carboxyl group of the ligand (e.g. in salicylate), usually abolishes or dramatically diminishes its ability to coordinate and thus to form fluorescent complexes. So, salicylate or similar compounds can be modified to become enzyme substrates as further exemplified below. The ternary Tb<sup>3+</sup> complexes are usually fluorescent at strongly alkaline pH, i.e. 12-13. At this pH, the aminopolycarboxylic acid ligand, e.g. EDTA, serves to chelate Tb<sup>3+</sup> with high affinity and keeps it soluble in water without the danger of hydroxide salt precipitation. Ligands like salicylate coordinate around Tb<sup>3+</sup> to form the ternary complex. After ligand excitation, the energy absorbed by the ligand is transferred to Tb<sup>3+</sup> by an internal energy transfer process.<sup>1</sup> Tb<sup>3+</sup> is then excited and subsequently fluoresce at characteristic wavelengths. The ternary complex between DTPA, Tb<sup>3+</sup>, and *p*-aminosalicylate (pAS)

\* To whom correspondence should be addressed at the Toronto Western Hospital.